JOURNAL OF CATALYSIS **116**, 171–183 (1989)

MoO_3 Catalysts Promoted by $MnMoO_4$

I. Synthesis, Characterization, and Selectivity in Oxidation of 1-Butene and 1,3-Butadiene to Maleic Anhydride

UMIT OZKAN,[1] ROBERT C. GILL,[2] AND MARIANNE R. SMITH

Department of Chemical Engineering, The Ohio State University, Columbus, Ohio 43210

Received April 21, 1988; revised November 1, 1988

MoO_3 catalysts impregnated with $MnMoO_4$ are active for the selective oxidation of C_4 hydrocarbons to maleic anhydride. Presence of $MnMoO_4$ creates a significant "promoter" effect in catalytic behavior of MoO_3. The pure phases and the impregnated catalysts have been characterized during various stages of their life history using characterization techniques such as X-ray diffraction, laser Raman spectroscopy, scanning electron microscopy, and BET surface area measurements, and their catalytic activity and selectivity in selective oxidation of 1-butene and 1,3-butadiene to maleic anhydride have been studied. © 1989 Academic Press, Inc.

INTRODUCTION

Simple molybdate catalysts containing nonstoichiometric ratios of molybdenum to metal have been the subject of several studies (*1–7*). These catalysts were observed to exhibit pronounced changes in their catalytic behavior as selective oxidation catalysts when this ratio (e.g., Mo/Co, Mo/Mg, etc.) was increased from that of the simple molybdate in its pure form. In a series of papers, Ozkan and Schrader have reported the catalytic activity of $NiMoO_4$ (*8–10*) and $CoMoO_4$ (*11*) catalysts with Mo to metal ratios larger than 1 : 1 in selective oxidation of C_4 hydrocarbons to maleic anhydride. Their characterization studies have revealed the two phase nature of these catalysts and identified MoO_3 surfaces which were in intimate contact with the simple molybdate phase as the active component which determined the selectivity to maleic anhydride.

In this study, the catalytic activity and selectivity of pure MoO_3 have been the focus of attention and its catalytic behavior has been modified by bringing its surfaces into close contact with $MnMoO_4$ through an impregnation procedure. The pure phases and the impregnated catalysts have been characterized using complementary characterization techniques and their catalytic activity and selectivity in selective oxidation of 1-butene and 1,3-butadiene to maleic anhydride have been studied.

This paper presents the results of the characterization studies as well as the activity and selectivity measurements over the pure phases and the impregnated catalysts in 1-butene and 1,3-butadiene oxidation. The second paper of this series will discuss the effect of temperature and oxygen partial pressure on product distribution and catalytic activity (*12*). The third paper (*13*) will present the results of transient response experiments on the same catalysts in the presence and absence of gas phase oxygen and will discuss oxygen insertion mechanisms and the catalytic job distribution among different components of the active catalyst.

EXPERIMENTAL

Catalyst Preparation

Precipitation of $MnMoO_4$. Manganese molybdate catalysts were prepared from

---

[1] To whom correspondence should be addressed.

[2] Present address: Mobil Oil Co., Paulsboro, NJ 08066.

0021-9517/89 $3.00
Copyright © 1989 by Academic Press, Inc.
All rights of reproduction in any form reserved.

aqueous solutions of manganese chloride (J. T. Baker, $MnCl_2 \cdot 4H_2O$) and ammonium heptamolybdate (Fisher, $(NH_4)_6Mo_7O_{24} \cdot 4H_2O$). A 0.4 *M* solution of molybdenum, in the form of ammonium heptamolybdate, was added dropwise to a 0.4 *M* solution of manganese chloride. During the addition, precipitation, and aging stages, the mixture was stirred vigorously. The temperature was maintained at 80°C using a temperature controller (Omega, Model 4001JC). Since the composition of simple molybdates has been previously shown to be extremely sensitive to the pH of the precipitation medium (*8*), the pH of the reaction mixture was carefully controlled and maintained at 6.0 by adding dilute HCl or NH_4OH as needed through a pH controller (Cole–Parmer, Model No. 5997-20). After aging for 3 h, the precipitation mixture was filtered. The precipitate was then washed with water and dried at 115°C for 12 h. The dried catalyst precursor was calcined under O_2 at 500°C for 4 h in quartz boats inside a tube furnace (Lindberg, Model 59544) equipped with a Eurotherm programmable temperature controller.

Impregnation of MoO_3 with $MnMoO_4$. Impregnated MoO_3 catalysts were prepared using a stepwise "wet impregnation" procedure. Molybdenum trioxide samples (Aldrich, MoO_3) were soaked in an aqueous suspension of manganese molybdate. The mixture, which contained carefully measured quantities of MoO_3 and $MnMoO_4$, was continuously stirred for 4 h. The impregnation period was followed by drying at 115°C for 4 h. This process was repeated until the desired ratio of $MnMoO_4$ to MoO_3 was achieved. The samples were then calcined under O_2 at 500°C for 4 h.

Characterization Techniques

Surface area. Surface areas of the catalyst samples were measured using a Micromeritics 2100E Accusorb instrument. Nitrogen was used as the adsorbate. Some measurements were repeated using krypton as the adsorbate.

Energy dispersive X-ray analysis. Compositional analyses of the catalyst samples were carried out using an energy dispersive X-ray analyzer (EDAX 9100). The characteristic X-ray lines used for the quantitative analysis were $K\alpha$ and L for manganese and molybdenum, respectively.

X-ray diffraction. X-ray powder diffraction patterns were obtained using a Scintag PAD V diffractometer automated by an ATT computer system. Cu$K\alpha$ radiation ($\lambda = 1.5432$ Å) was used as the incident X-ray source.

Laser Raman spectroscopy. Raman spectra were obtained using a Spex 1403 laser Raman spectrometer equipped with a Datamate microprocessor for data collection and processing. The 514.5-nm line of a 5-W Ar ion laser (Spectra Physics) was used as the excitation source. The laser power was 30 mW, and a scanning time of 0.7 sec/cm^{-1} was used. The slits were set at 3 cm^{-1}.

Scanning electron microscopy. Scanning electron microscopy studies were conducted using a Hitachi S-510 scanning electron microscope. Powdered samples were placed on cylindrical sample mounts which were coated with wet carbon black for adhesion. The samples were then sputter coated with approximately 200 Å of gold to prevent charging under the electron beam. The micrographs were typically taken by using a 90-amp current at 25 kV and a working distance of 24 mm.

Catalytic Activity and Selectivity Measurements

Selective oxidation reaction experiments were performed using a fixed-bed, integral reactor. The cylindrical reactor was made out of 304 stainless steel. Its length was 13.5 in. and its diameter was 0.742 in. The reactor contained 11 thermocouples to monitor the internal temperature profile. The type K thermocouples (Omega Engineering), covered with 0.040-in.-diameter stainless-steel sheaths, were inserted through the wall of the reactor, allowing the sensing tips to be placed at different axial and radial positions. The reactor and the feed preheater were immersed inside a fluidized sand bath (Techne FB-08) for thermal stability.

The top and bottom $1\frac{1}{2}$-in. portions of the bed were filled with silicon carbide (Norton Co., size 8 crystalline SiC). The catalyst bed consisted of a homogeneous mixture of catalyst pellets and SiC particles. The reaction runs were performed using a constant total surface area of catalyst in the bed (30 m^2). In the reaction runs that were performed to assess the effect of conversion on selectivity, the total surface area was adjusted to achieve the same conversion level for each catalyst.

The composition and the flow rate of the feed gas mixture was controlled using mass flow controllers (Tylan FC260) which were calibrated specifically for each of the gases.

The feed and reaction products were analyzed using an analytical system which consisted of two gas chromatographs (Hewlett–Packard 5890A) equipped with thermal conductivity and flame ionization detectors. The feed, the reactor, and the analytical systems have been previously described in detail by Gill (*14*). The operating conditions which were kept constant for the studies reported in this article were as follows: reactor pressure, 5 psig; reaction temperature, 480°C; hydrocarbon concentration (by volume) in the feed mixture, 2.40%; oxygen concentration, 19.52%; nitrogen concentration, 78.08%; volumetric flow rate of hydrocarbon, 738 cm^3(STP)/h; total molar flow rate, 1.37 gmol/h.

The percentage conversion of the feed hydrocarbon is defined as

$$\frac{\text{mol of HC consumed}}{\text{mol of HC in feed}} \times 100\%,$$

where HC is either 1-butene or 1,3-butadiene.

The percentage selectivity to product *A* is defined as

$$\frac{\text{mol of } A \text{ produced}}{\text{mol of HC consumed}} \times \frac{1}{\gamma} \times 100\%,$$

where γ is the ratio of number of C atoms in the reactant to the number of C atoms in the product.

The yield of product *A* is defined as

$$\frac{\text{mol of } A \text{ produced}}{\text{mol of HC in feed}} \times \frac{1}{\gamma} \times 100\%.$$

RESULTS

Catalyst Characterization

The surface area measurements for the pure phases and the impregnated catalysts with various compositions are presented in Table 1. Compositional analysis of the Mn MoO_4 catalyst, obtained by energy dispersive X-ray analysis technique, showed a 1 : 1 ratio of Mn : Mo, indicating that there were no detectable impurities in the compound.

The *d*-spacings obtained from X-ray diffraction pattern of pure MoO_3 were found to agree with those reported earlier in the literature (*15*). The *d*-spacings of $MnMoO_4$ were in agreement with the data reported in JCPDS files (*16*). The impregnated sample exhibited a pattern identical to that of MoO_3. It was not possible to identify peaks corresponding to $MnMoO_4$ in this pattern since the most intense peaks of $MnMoO_4$ (3.45 Å) and MoO_3 (3.46 Å) almost coincided with each other.

Laser Raman spectroscopy was used for characterization of the catalysts during various stages of preparation. Figure 1 shows Raman spectra of $MnMoO_4$ as precursor

TABLE 1

Surface Areas of Pure MoO_3, Pure $MnMoO_4$, and the Impregnated Catalysts

Catalyst	Surface area (m^2/g)
MoO_3	2.1
$MnMoO_4$	1.7
$MnMoO_4/MoO_3 = 0.08$	1.9
$MnMoO_4/MoO_3 = 0.15$	2.4
$MnMoO_4/MoO_3 = 0.30$	2.2

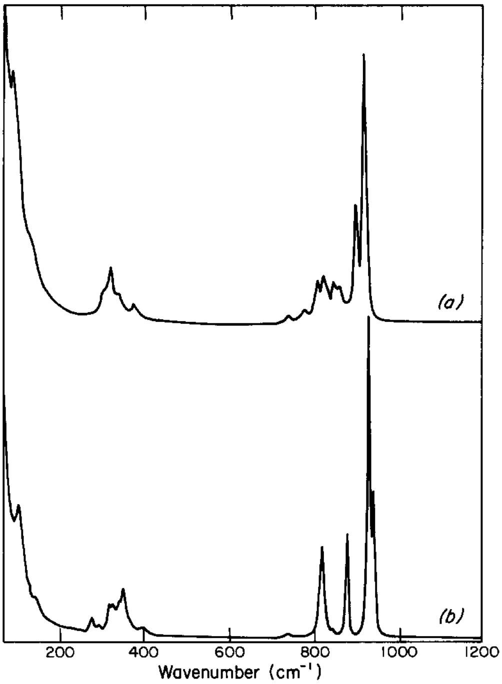

FIG. 1. Raman spectra of (a) $MnMoO_4$ precursor (before calcination) and (b) $MnMoO_4$ (after calcination).

(spectrum a) and as active catalyst (spectrum b). Change in the spectra is due to loss of crystal water and ammonia during the calcination step and to crystallization of the catalyst to attain its final lattice structure.

Figure 2 presents a comparison of the Raman spectra of MoO_3 (a), impregnated MoO_3 (b), and $MnMoO_4$ (c). The Raman bands that correspond to $MnMoO_4$ (880, 930, 942 cm^{-1}), although weak in intensity, are clearly visible. The position and relative intensity of MoO_3 Raman bands do not exhibit any changes. Table 2 lists the band positions for MoO_3, $MnMoO_4$, and MoO_3 impregnated with $MnMoO_4$.

Figure 3 shows Raman spectra of MoO_3 impregnated with different quantities of $MnMoO_4$, with $MnMoO_4/MoO_3$ molar ratio ranging from 5.6 to 30%. The bands at 880, 930, and 942 cm^{-1} increase in intensity with increasing molar ratios of $MnMoO_4$ to MoO_3.

Scanning electron microscopy studies provided visual information about the nature of impregnated MoO_3 catalysts. Scan-

TABLE 2

Raman Bands of MoO_3, $MnMoO_4$, and MoO_3 Impregnated with $MnMoO_4$

Catalyst	0–200	200–400	400–600 (cm^{-1})	600–800	800–1000	1000+
MoO_3	82 m 93 w 115 s 128 m 157 m 198 w	271 w 245 w 283 s 291 m 337 m 364 w 378 m	471 w	666 s	819 vs 995 vs	
$MnMoO_4$	94 vw 144 vw	277 vw 298 vw 325 w 331 w 354 w		743 vs	821 m 879 m 929 vs 940 s	
MoO_3 impregnated with $MnMoO_4$ ($MnMoO_4/MoO_3$ = 0.15)	81 w 97 vw 114 s 127 m 156 m 196 vw	215 vw 243 vw 282 s 290 m 336 vw 364 vw 377 vw	469 vw	665 w	818 vs 881 vw 930 vw 942 vw 994 vs	

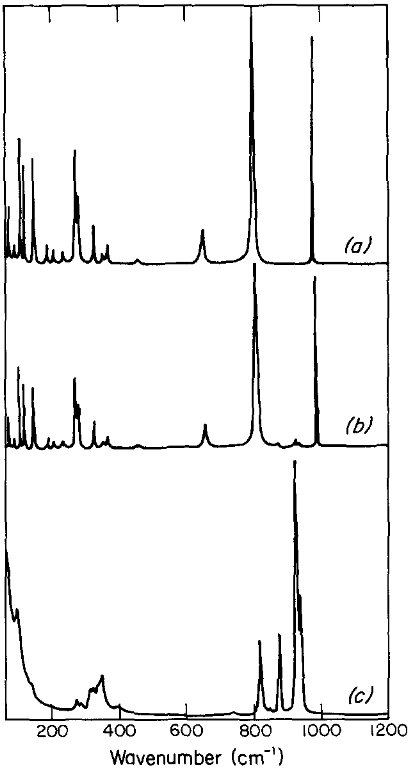

FIG. 2. Raman spectra of (a) MoO_3, (b) MoO_3 impregnated with $MnMoO_4$, and (c) $MnMoO_4$.

ning electron micrographs obtained from pure MoO_3 samples were similar to the ones reported in a previous study (*8*). MoO_3 crystallites were observed to be characterized by well-defined hexagonal shapes, sharp edges and corners, and smooth crystal face surfaces (Fig. 4a). Scanning electron micrographs obtained from $MnMoO_4$ samples exhibited particles smaller in size and less regular in shape (Fig. 4b). They were also observed to form large clusters. Figures 5 and 6 show scanning electron micrographs taken from impregnated MoO_3 catalyst with a $MnMoO_4/MoO_3$ molar ratio of 0.15. Several interesting phenomena about the nature of the impregnated catalyst are observed in these micrographs. First, two distinct phases coexisting are clearly visible. $MnMoO_4$ crystallites are seen to be in a more dispersed state than the large agglomerates they formed in pure $MnMoO_4$. Second, the two phases are in intimate contact with each other.

Activity and Selectivity Measurements

Oxidation of 1-butene. Selective oxidation experiments were conducted over pure phases (MoO_3 and $MnMoO_4$) and impregnated catalysts with different $MnMoO_4/MoO_3$ mole ratios using 1-butene as the starting material. The first phase of experiments was performed using equal surface areas of catalysts in the reactor. The species detected in the product stream included unconverted 1-butene, *cis*-2-butene, *trans*-2-butene, 1,3-butadiene, furan, acrolein, maleic anhydride, carbon oxides, and small quantities of cracking products.

The percentage selectivities to various reaction products and intermediates and

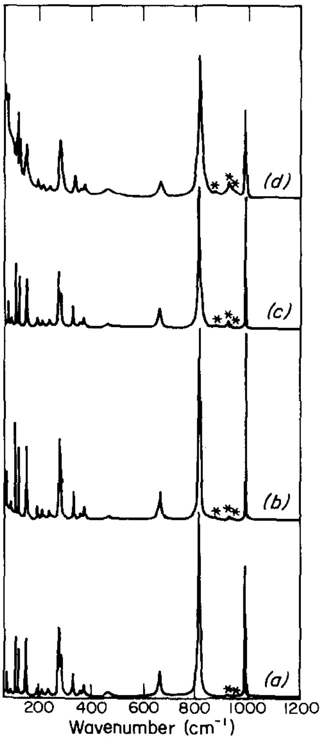

FIG. 3. Raman spectra of MoO_3 impregnated with $MnMoO_4$ (a) $MnMoO_4/MoO_3$ = 0.056, (b) $MnMoO_4/MoO_3$ = 0.083, (c) $MnMoO_4/MoO_3$ = 0.150, and (d) $MnMoO_4/MoO_3$ = 0.300. *$MnMoO_4$.

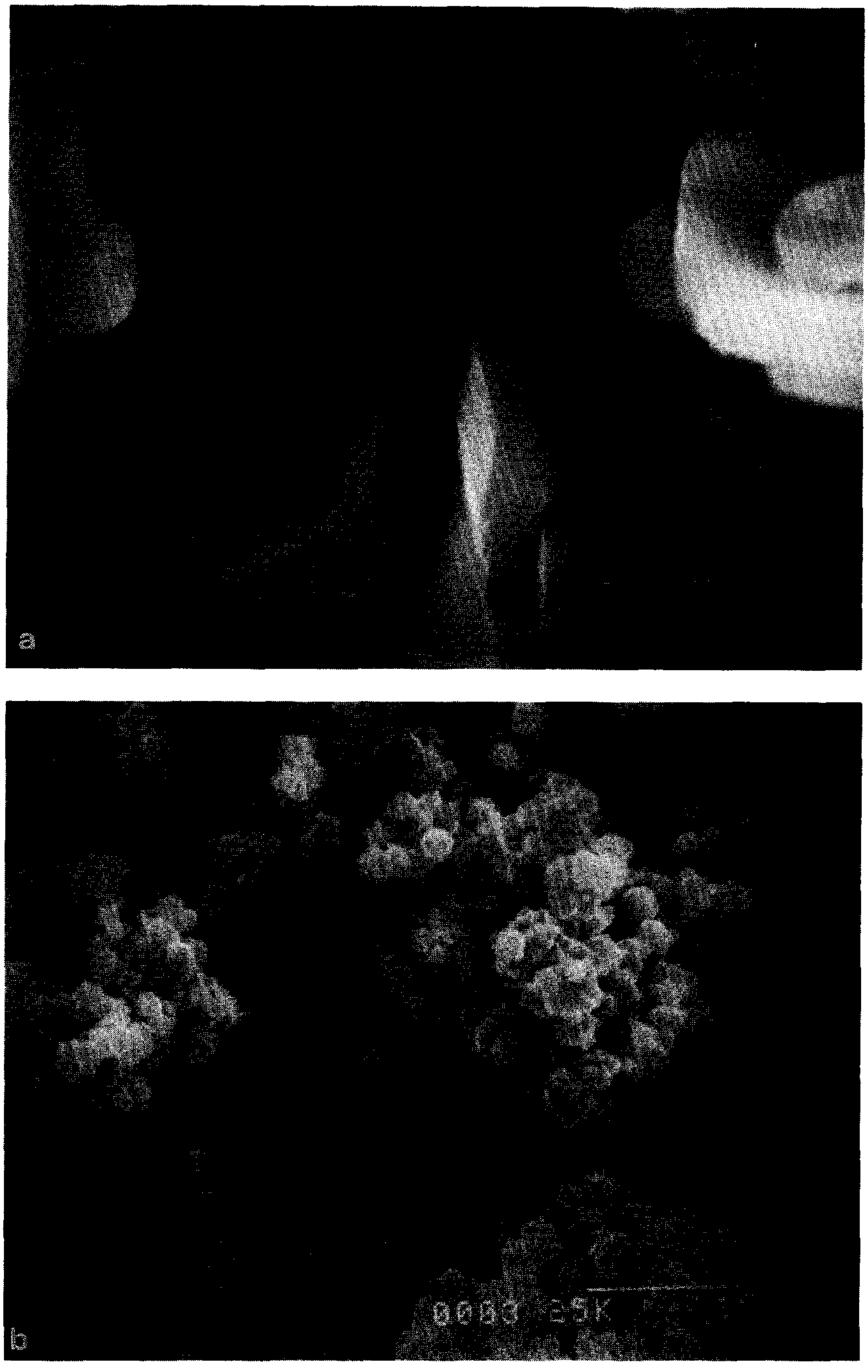

FIG. 4. Scanning electron micrographs of (a) pure MoO_3 and (b) pure $MnMoO_4$.

percentage hydrocarbon consumed are presented in Table 3. The most striking aspect of the conversion data is the difference between the maleic anhydride yields of the pure phases and the impregnated catalysts. The pure manganese molybdate catalyst is

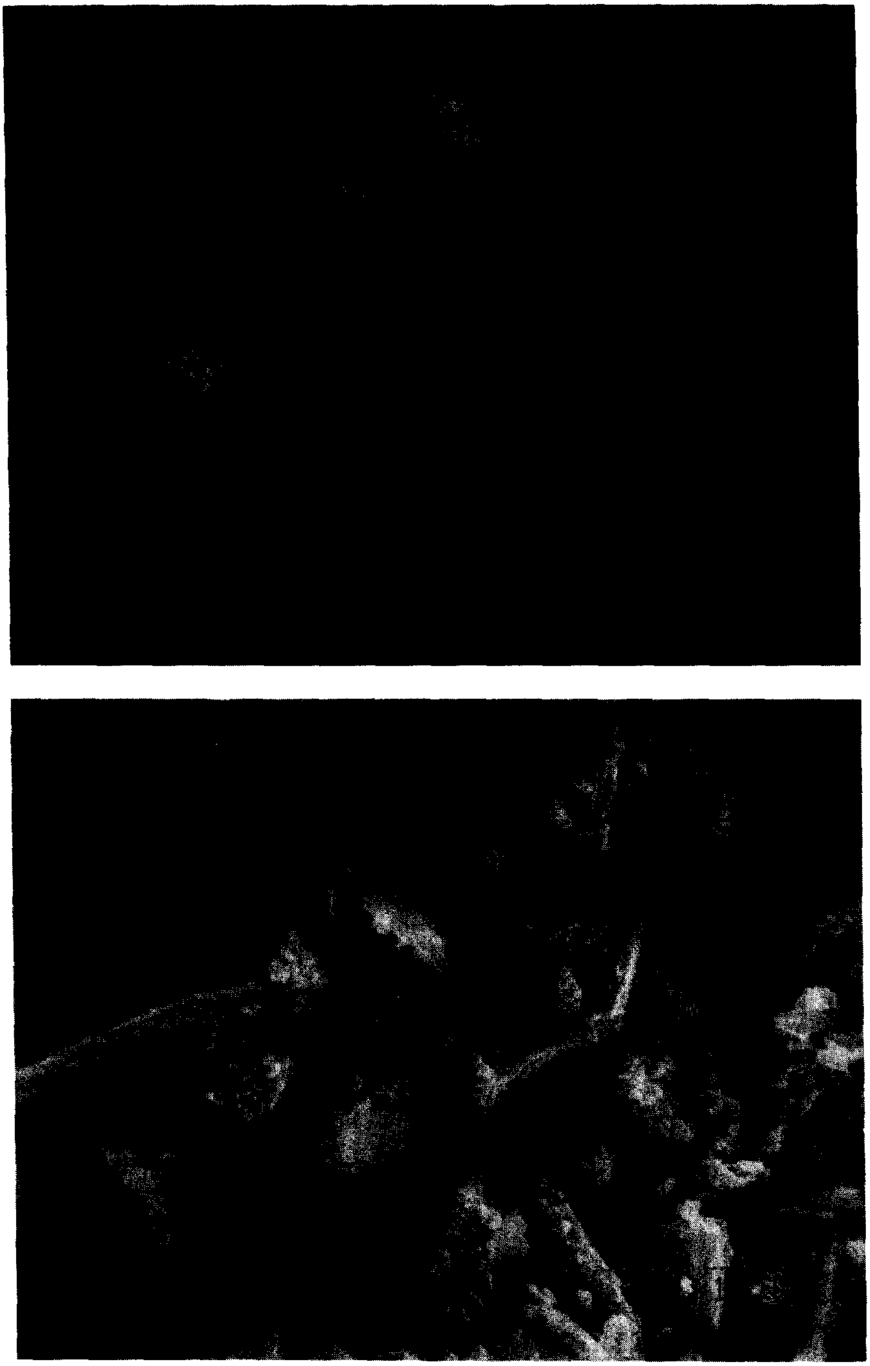

FIG. 5. Scanning electron micrographs of MoO_3 catalysts impregnated with $MnMoO_4$ ($MnMoO_4/MoO_3 = 0.15$).

observed to produce no maleic anhydride. The pure molybdenum trioxide catalyst is capable of converting the hydrocarbon feed to maleic anhydride in small quantities; but substantial yields of maleic anhydride are achieved over the impregnated catalyst

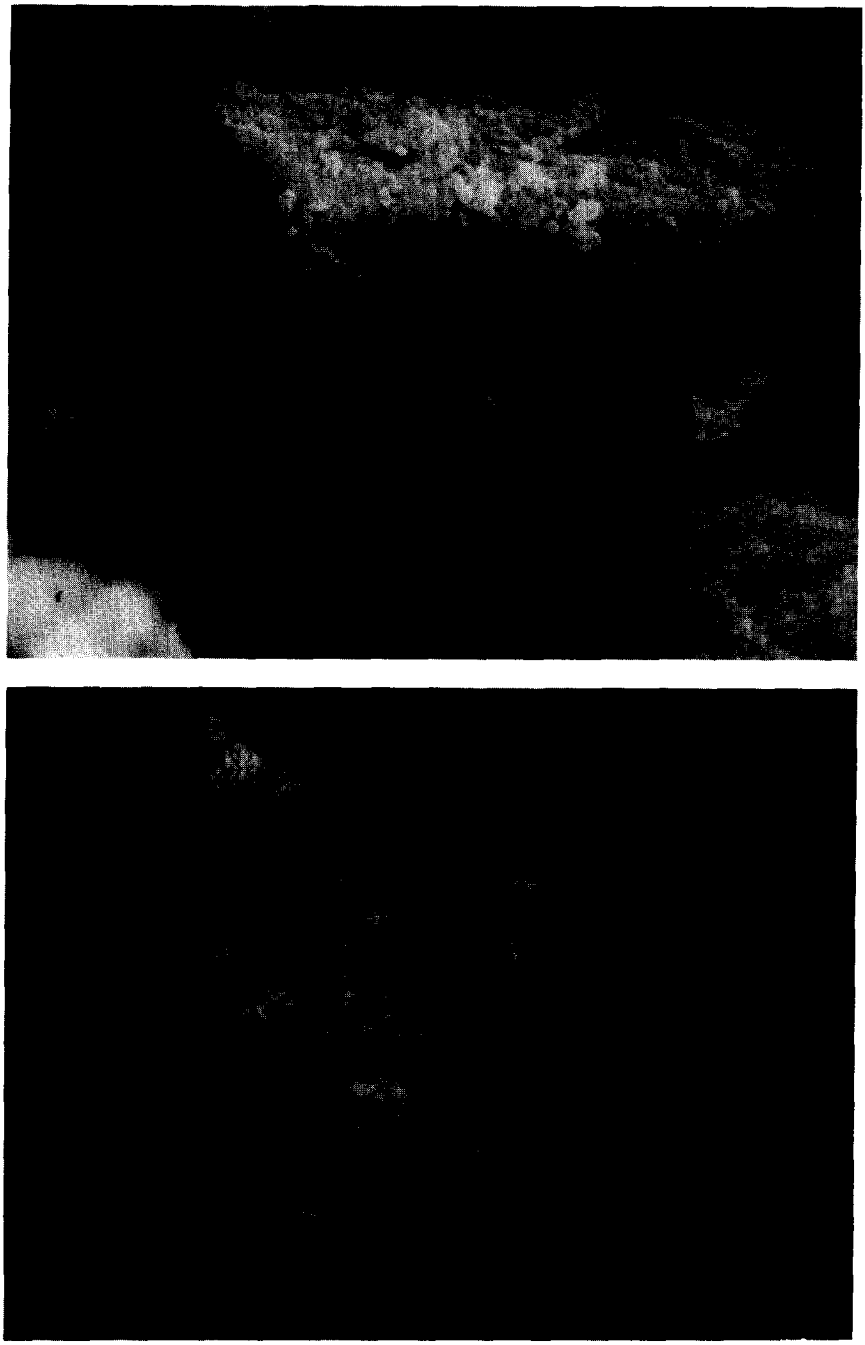

FIG. 6. Scanning electron micrographs of MoO_3 catalyst impregnated with $MnMoO_4$ ($MnMoO_4/MoO_3$ = 0.15).

(~38%). A comparison of the selectivities exhibits the same phenomenon much more pronouncedly. The pure phases, MoO_3 and $MnMoO_4$, have selectivities of 10.9 and 0.0%, respectively, whereas the impregnated catalysts show selectivities around 51–52%.

Figure 7 shows the variation of selectiv-

TABLE 3

Variation of Selectivities with Catalyst Composition in 1-Butene Oxidation

% Selectivity	MoO_3	$MnMoO_4/MoO_3 = 0.08$	$MnMoO_4/MoO_3 = 0.30$	$MnMoO_4$
1,3-Butadiene	43.8	1.7	1.0	23.7
Furan	3.3	0.2	0.1	1.8
Maleic anhydride	10.9	50.8	51.7	0.0
Acrolein	3.8	2.8	1.9	2.5
Carbon oxides	26.8	41.6	42.0	67.4
% Hydrocarbon consumed	10.5	73.6	73.6	45.9

ity ratios (% selectivity to maleic anhydride/% selectivity to CO_x) with catalyst composition in 1-butene oxidation. This ratio is much smaller than unity for the pure phases (0.0 and 0.4 for $MnMoO_4$ and MoO_3, respectively), but it is larger than unity for all of the impregnated catalysts indicating that the impregnated catalysts are capable of producing more maleic anhydride than complete oxidation products, whereas this behavior is just the opposite for the pure components.

To assess the effect of conversion on the selectivity levels, a series of experiments were performed where the overall conversion levels were kept constant by adjusting the amount of total surface area of the catalyst present in the reactor. Figure 8 shows a comparison of selectivities to maleic anhydride and to complete oxidation products at constant conversion levels of 40 and 50%. It is shown that at both conversion levels, $MnMoO_4$ exhibits no selectivity for maleic anhydride and more than 90% of the conversion is to complete oxidation products. The MoO_3 has a selectivity of ~12% to maleic anhydride, but its selectivity to complete oxidation products is about five times higher. The impregnated catalyst is more selective to maleic anhydride and less selective to complete oxidation products than either of the two pure phases at both conversion levels.

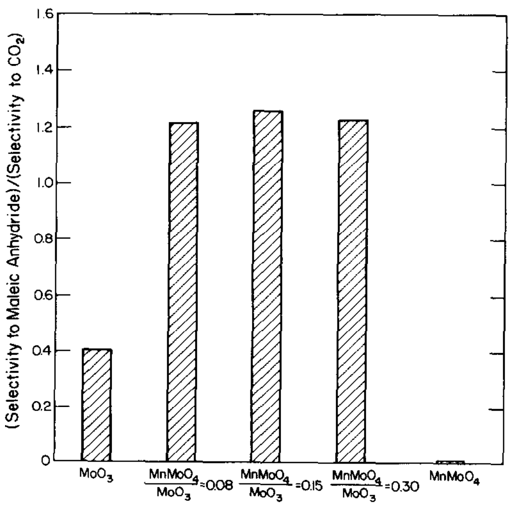

FIG. 7. Variation of selectivity ratios with catalyst composition for 1-butene oxidation.

Oxidation of 1,3-butadiene. 1,3-Butadiene is generally accepted as an intermediate in the reaction pathway from 1-butene to maleic anhydride. Selective oxidation experiments were repeated after switching to 1,3-butadiene as the feed material. Comparison of percentage selectivities to various reaction products obtained by using equal total catalyst surface areas is presented in Table 4. The overall conversion of 1,3-butadiene appears to be higher than that of 1-butene for every catalyst sample. The major reaction product over both of the pure phases is seen to be CO_x, whereas the impregnated catalysts are observed to produce maleic anhydride as the major reaction product (~55% conversion).

Figure 9 shows variation of selectivity ratios (% selectivity to maleic anhydride/% selectivity to CO_x) with catalyst composition for 1,3-butadiene oxidation. $MnMoO_4$ shows no conversion to maleic anhydride and has a selectivity of ~87% to CO_x. Pure

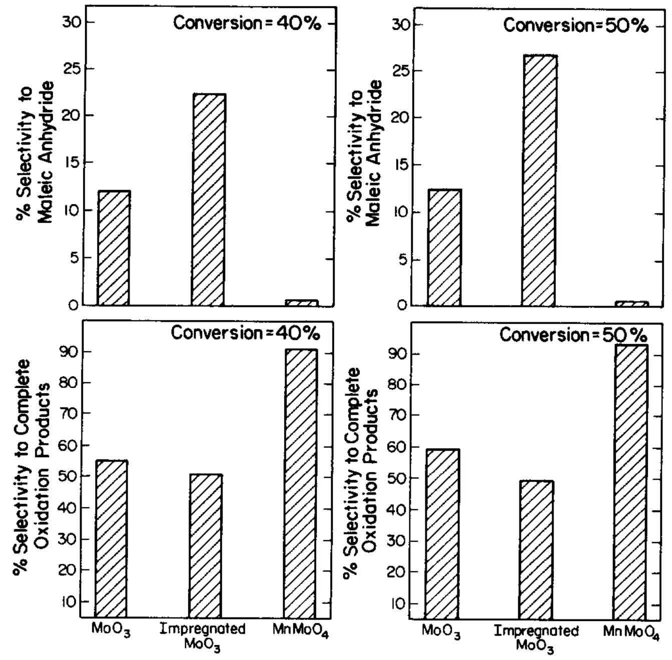

FIG. 8. Comparison of selectivities at equal conversion levels in 1-butene oxidation.

MoO_3 gives a considerable yield of maleic anhydride, but conversion to CO_x is much more dominant. The selectivity ratios for the impregnated catalysts are all above one, exhibiting at least 50% more selectivity to maleic anhydride than they have for complete oxidation products. It is also observed that the ratio of $MnMoO_4$ to MoO_3 in the impregnated catalyst does not have a strong effect on selectivities in the range which is used in this study.

Stability of catalysts. To evaluate the stability of catalysts over prolonged reaction times, the selective oxidation experiment of 1-butene over an impregnated MoO_3 catalyst ($MnMoO_4/MoO_4$ = 0.15) was continued for 2 days. No significant decay was observed in the catalytic behavior over this time period. Figure 10 shows variation of selectivities to maleic anhydride, CO_x, 1,3-butadiene, and furan during the first 24 h of the reaction.

DISCUSSION

Although simple molybdate catalysts with "excess MoO_3" have been the subject of various studies, MoO_3 catalysts promoted by simple molybdates have not been

TABLE 4

Variation of Selectivities with Catalyst Composition in 1,3-Butadiene Oxidation

% Selectivity	MoO_3	$MnMoO_4/MoO_3$ = 0.08	$MnMoO_4/MoO_3$ = 0.30	$MnMoO_4$
Furan	15.2	0.1	0.1	2.3
Acrolein	15.5	3.7	1.7	3.2
Maleic anhydride	23.5	56.3	57.1	0.0
Carbon oxides	31.5	36.5	38.4	87.2
% Hydrocarbon consumed	33.2	96.9	95.4	68.5

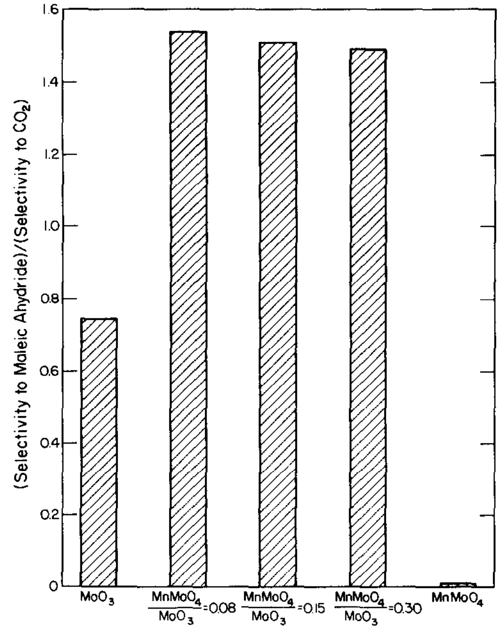

FIG. 9. Variation of selectivity ratios with catalyst composition for 1,3-butadiene oxidation.

studied extensively. Since MoO_3 crystal surfaces were previously shown to catalyze both complete oxidation and selective oxidation reactions (*8–11*), this study has focused on catalytic behavior of MoO_3 modified by being brought into close contact with $MnMoO_4$.

A careful control of synthesis parameters was necessary to ensure the purity of the synthesized $MnMoO_4$ sample since earlier studies have shown the sensitivity of the composition of simple molybdates to the conditions during synthesis procedure and how, in turn, the composition of simple molybdates could drastically change their catalytic behavior. The $MnMoO_4$ samples which were prepared at a pH of 6 and a temperature of 80°C were shown to be free of excess MoO_3. The MoO_3 samples impregnated with pure $MnMoO_4$ clearly showed the presence of two distinct phases through scanning electron microscopy and laser Raman spectroscopy. Scanning electron microscopy provided visual evidence for the coexistence of MoO_3 and $MnMoO_4$ phases. $MnMoO_4$ was observed to be in a more dispersed state in the impregnated sample than it was in the pure $MnMoO_4$ sample. Laser Raman spectra showed an increase in $MnMoO_4$ bands proportional to

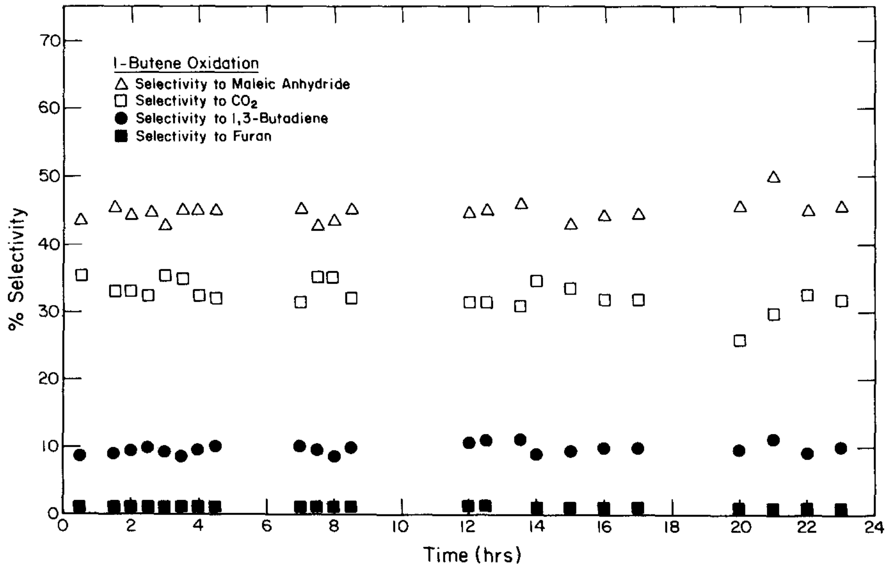

FIG. 10. Variation of selectivity with time in 1-butene oxidation over impregnated catalyst ($MnMoO_4/MoO_3$ = 0.15).

their percentage in the impregnated sample. No change was observed in the lattice structure of MoO_3 due to impregnation.

A comparison of catalytic behavior of the pure phases (MoO_3 and $MnMoO_4$) with that of the impregnated catalysts showed that presence of $MnMoO_4$ in close contact with MoO_3 created a "promoter" effect on the catalytic performance of MoO_3. The selectivity of MoO_3 to maleic anhydride improved significantly as a result of impregnation with $MnMoO_4$ although $MnMoO_4$ showed no selectivity to maleic anhydride in pure form. The same phenomenon was observed in all experiments carried out over a wide range of temperature, oxygen partial pressure, and conversion (*12*). This result differs significantly from those published previously by Trifiro *et al.* (*17*) who reported considerable selectivity to maleic anhydride over $MnMoO_4$ catalysts. Since presence of small quantities of excess MoO_3 is known to change the catalytic behavior of simple molybdates dramatically (*9, 11*), this difference may be due to presence of MoO_3 in their samples. It is not, however, possible to draw any definite conclusions about the presence of MoO_3 without data obtained from a detailed characterization of the catalyst with Raman spectroscopy, a technique which is very sensitive in detecting small quantities of MoO_3.

The reaction pathway appears to include 1,3-butadiene and furan as possible reaction intermediates which is an observation that agrees with the findings previously published in the literature. Comparison of the yields in 1-butene and 1,3-butadiene oxidation shows that bypassing the oxidative dehydrogenation step causes a much more pronounced increase in maleic anhydride yield over MoO_3 (an ~6.5-fold increase) than it does over the impregnated catalyst (an ~1.4-fold increase). This result seems to suggest that one of the important functions of $MnMoO_4$ in maleic anhydride formation is promotion of the oxidative dehydrogenation of 1-butene to 1,3-butadiene. This observation agrees with earlier reports where a similar catalytic role was attributed to nickel molybdate and cobalt molybdate (*10, 11*). The data also suggest that complete oxidation of the reactant and the intermediates takes place at significant levels. Presence of cracking products (C_1, C_2, C_3) and acrolein in the product stream signals presence of cracking reactions in the reaction scheme followed by partial and possibly complete oxidation.

The comparison of selectivities at equal conversion levels provides significant evidence about the promoter effect of Mn MoO_4 on catalytic behavior of MoO_3, since the pronounced increase in maleic anhydride yield which is accompanied by a considerable reduction in complete oxidation is clearly demonstrated through these sets of data.

The relationship between the promoter effect observed in this study and the catalytic job distribution among different components of the active catalyst will be established in the next papers in this series.

ACKNOWLEDGMENTS

The financial support from U.S. DOE through Battelle Northwest Pacific Laboratories, from AMAX Foundation, and from ACS Petroleum Research Fund is gratefully acknowledged. The authors also thank Mr. Reinaldo A. Hernandez for his assistance in scanning electron microscopy work.

REFERENCES

1. Hartig, M. J. D., U.S. Patent 2,625,519 (Jan. 13, 1953).
2. Grzybowska, B., and Mazurkiewicz, A., *Bull. Acad. Pol. Sci. Ser. Sci. Chim.* **27**(2), 141 (1979).
3. Grzybowska, B., and Mazurkiewicz, A., *Bull. Acad. Pol. Sci. Ser. Sci. Chim.* **27**(2), 149 (1979).
4. Grzybowska, B., Haber, J., and Janas, J., *J. Catal.* **49,** 150 (1977).
5. Oganowski, W., Hanuza, J., Jezowska-Trzebiatowska, B., and Wrzyszcz, J., *J. Catal.* **39,** 161 (1975).
6. Mazzocchia, C., Del Rosso, R., and Centola, P., *in* "Proceedings, 5th Ibero-American Symposium on Catalysis, Lisbon, Portugal, 1979."
7. Mann, R. S., and Hahn, K. W., *J. Catal.* **15,** 329 (1969).
8. Ozkan, U., and Schrader, G. L., *J. Catal.* **95,** 120 (1985).

9. Ozkan, U., and Schrader, G. L., *J. Catal.* **95,** 137 (1985).

10. Ozkan, U., and Schrader, G. L., *J. Catal.* **95,** 147 (1985).

11. Ozkan, U., and Schrader, G. L., *Appl. Catal.* **23,** 327 (1986).

12. Gill, R. C., and Ozkan, U., submitted for publication.

13. Moctezuma, E., and Ozkan, U., submitted for publication.

14. Gill, R. C., M.S. thesis, The Ohio State Univ., August 1987.

15. Kihlborg, L., *Acta Chem. Scand.* **13,** 954 (1959).

16. Abrahams, S. C., and Reddy, J. M., *J. Chem. Phys.* **43,** 2533 (1965).

17. Trifiro, F., Banfi, C., Caputo, G., Forzathi, P., and Pasquon, I., *J. Catal.* **30,** 393 (1973).